



**HAL**  
open science

## Characterization of Optical and Structural of Lanthanum Doped LiTaO<sub>3</sub> Thin Films

Irzaman Irzaman, Yunus Pebriyanto, Epa Rosidah Apipah, Iman Noor,  
Ahmad Alkadri

► **To cite this version:**

Irzaman Irzaman, Yunus Pebriyanto, Epa Rosidah Apipah, Iman Noor, Ahmad Alkadri. Characterization of Optical and Structural of Lanthanum Doped LiTaO<sub>3</sub> Thin Films. *Integrated Ferroelectrics*, 2015, 167 (1), pp.137-145. 10.1080/10584587.2015.1107358 . hal-01864899

**HAL Id: hal-01864899**

**<https://hal.science/hal-01864899>**

Submitted on 30 Aug 2018

**HAL** is a multi-disciplinary open access archive for the deposit and dissemination of scientific research documents, whether they are published or not. The documents may come from teaching and research institutions in France or abroad, or from public or private research centers.

L'archive ouverte pluridisciplinaire **HAL**, est destinée au dépôt et à la diffusion de documents scientifiques de niveau recherche, publiés ou non, émanant des établissements d'enseignement et de recherche français ou étrangers, des laboratoires publics ou privés.

# Characterization of Optical and Structural of Lanthanum Doped LiTaO<sub>3</sub> Thin Films

IRZAMAN,<sup>1,\*</sup> YUNUS PEBRIYANTO,<sup>2</sup> EPA ROSIDAH  
APIPAH,<sup>2</sup> IMAN NOOR,<sup>2</sup> AND AHMAD ALKADRI<sup>3</sup>

<sup>1</sup>Lecturer in Department of Physics, Bogor Agricultural University, Indonesia <sup>2</sup>Graduate Student of Biophysics Program, Bogor Agricultural University, Indonesia

<sup>3</sup>Graduate Student of Forest Products Science and Technology, Bogor Agricultural University, Indonesia

*Undoped, 5%, and 10% lanthanum doped lithium tantalate thin films were annealed at 550°C temperature for 12.5 hours and their properties were characterized. The results showed that the dopant addition affects the crystal formation of LiTaO<sub>3</sub>, especially the 10% La<sub>2</sub>O<sub>5</sub> dopant, where the lattice of  $a = 5.11 \text{ \AA}$ ,  $c = 13.30 \text{ \AA}$ , and its crystal was hexagonal. The observed functional groups were O-H, N-H, C = C, Li-O, Ta-O. The higher La<sub>2</sub>O<sub>5</sub> dopant concentration leads to the higher absorption of Ta-O and Li-O, the lower the energy gap, the higher the refractive index, and the smaller the particle size of thin films.*

**Keywords** Lithium tantalite; lanthanum dopant; optical properties; structure; thin films

## 1. Introduction

Development of Lithium Tantalate (LiTaO<sub>3</sub>) films can be carried out by using various methods, such as Chemical Solution Deposition (CSD), Metal Organic Chemical Vapor Deposition (MOCVD), rf sputtering, and Pulsed Laser Ablation Deposition (PLAD) [1], and it does not need complicated treatment [1,2]. LiTaO<sub>3</sub> is one of the widely used optoelectric materials to its ferroelectric, piezoelectric, and pyroelectric properties [1,3-8,15-16,]. It is also an attractive materials for integrated-optic applications due to its nonlinear optical properties [9-13], large electrooptic and piezoelectric coefficient and its superior resistance to laser-induced optical damage [16-19,24,35,37,38,44]. In other hand, it is a ferroelectric crystal which undergoes high Curie temperature of 608 °C and it also has high melting temperature at 1650 °C [34].

However, most of the techniques used to make LiTaO<sub>3</sub> are not only expensive but also involve difficult stoichiometric quantification and complex equipment. Sol-gel processing [10], a solution-based method, is interesting due to its ease of production and lower cost, and large area thin film. However, the commonly used alkoxide precursors to produce

LiTaO<sub>3</sub> films by sol-gel method are highly reactive and require careful control of the hydrolysis-condensation reaction [3].

In this research, LiTaO<sub>3</sub> thin films were coated on p-type silicon substrates by using CSD method, followed by spin-coating technique and annealed at the temperature of 550°C then characterized using X-Ray Diffraction (XRD), Fourier Transform Infrared Spectroscopy (FTIR), UV-Vis Wave Analyzer, and Particle Size Analyzer (PSA). This research aims to manufacture the lanthanum doped LiTaO<sub>3</sub> thin films and determine its optical and structural properties.

## 2. Experimental

The thin films preparation was started by cutting the Si substrate with the size of 8 mm × 8 mm, each as many as 5 pieces. Then, the substrates were cleaned using aqua bidest and dried [35,37,45]. In this case, three LiTaO<sub>3</sub> solutions were prepared using CSD (Chemical Solution Deposition) method. The first solution was prepared by mixing 0.1650 gram of LiCH<sub>3</sub>COO and 0.5524 gram of Ta<sub>2</sub>O<sub>5</sub> which were soluted inside 2.5 ml of 2-metoxy methanol which called undoped LiTaO<sub>3</sub> solution. The second solution was prepared by mixing 0.1650 gram of LiCH<sub>3</sub>COO and 0.5524 gram of Ta<sub>2</sub>O<sub>5</sub> which were soluted LiTaO<sub>3</sub> 2.5 ml of 2-metoxy methanol with the addition of 0.0295 gram of La<sub>2</sub>O<sub>5</sub> as dopant which called 5% lanthanum doped LiTaO<sub>3</sub> solution. Afterwards, the third solution was prepared by mixing 0.1650 gram of LiCH<sub>3</sub>COO and 0.5524 gram of Ta<sub>2</sub>O<sub>5</sub> which were soluted inside 2.5 ml of 2-metoxy methanol with the addition of 0.0590 gram of La<sub>2</sub>O<sub>5</sub> which called 10% lanthanum doped LiTaO<sub>3</sub> solution.

After the preparation of those three solutions, they were sonificated for 90 minutes using Branson 2510. Afterwards, the solution was dropped towards the substrate's surface on spin coating rotator with speed of 3000 rpm, conducted twice. The remaining solution then dried at 80°C for 24 hours, then characterized using FTIR and PSA. The dropped substrate was then annealed using Furnace with the increasing rate of temperature at 1.7°C/minute, started from room temperature until it reaches 550°C and held constantly for 12.5 hours, and then cooled down into room temperature. The formed thin films were characterized using XRD and Optical Ocean USB 2000.

## 3. Results and Discussion

### 3.1 XRD Pattern

Figure 1 shows the XRD pattern of LiTaO<sub>3</sub> thin films with p-type Si (100) substrate after annealing at 550°C. The data were obtained with interval of 0.02° in the range of 20°–80° [32,33]. These three patterns show a peak at  $2\theta = 70^\circ$  because the used substrate is silicon.

XRD pattern shows that LiTaO<sub>3</sub> thin films have both crystalline and amorphous structures. Undoped LiTaO<sub>3</sub> thin films have mixed structure with lattice parameter of  $a = 5.13 \text{ \AA}$  and  $c = 13.54 \text{ \AA}$ . Meanwhile, for 5% La doped LiTaO<sub>3</sub> thin films, the structure is not significantly different with the undoped. However, it has smaller lattice parameter of  $a = 4.92 \text{ \AA}$  and  $c = 14.19 \text{ \AA}$ . Moreover, for 10% La<sub>2</sub>O<sub>5</sub> doped LiTaO<sub>3</sub> thin films, there is a peak (crystalline) of LiTaO<sub>3</sub> with lattice parameter of  $a = 5.11 \text{ \AA}$  and  $c = 13.30 \text{ \AA}$ .

Decreasing in crystal size is also influenced by the radii of its constituent ions. Ionic radii of Li<sup>+</sup>, Ta<sup>5+</sup> and La<sup>3+</sup> are 0.90 Å, 0.78 Å and 1.172 Å, respectively. It can be seen that the ionic radius of La<sup>3+</sup> is closer to that of Li<sup>+</sup> so that La<sup>3+</sup> can occupy the positions of

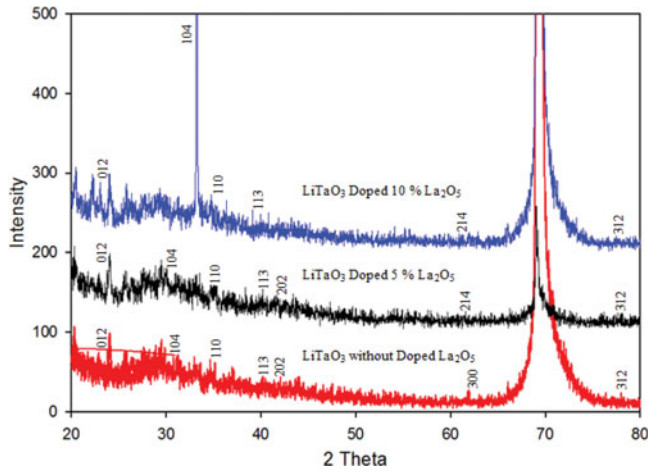


**Figure 1.** the XRD pattern of  $\text{LiTaO}_3$  thin film with p type Si (100) substrate after annealing at  $550^\circ\text{C}$ .

$\text{Li}^+$  in the crystal structure. The difference of Ionic radii between dopant and replaced ion affects the formation of spinel phase. This leads to crystal size decreasing which is caused by the existence of dopant cations in the structure of  $\text{LiTaO}_3$ .

### 3.2. FTIR Results

The results show the existence of stretching vibration of OH group, C = C aromatic bonding, Li-O bonding, and Ta-O bonding at wave numbers of  $3100\text{--}3900\text{ cm}^{-1}$ ,  $1650\text{--}1450\text{ cm}^{-1}$ ,  $1440\text{--}1420\text{ cm}^{-1}$ , and  $610\text{--}945\text{ cm}^{-1}$ , respectively [29]. According to these results, it is implied that there is a change in absorbance value of  $\text{LiTaO}_3$  for

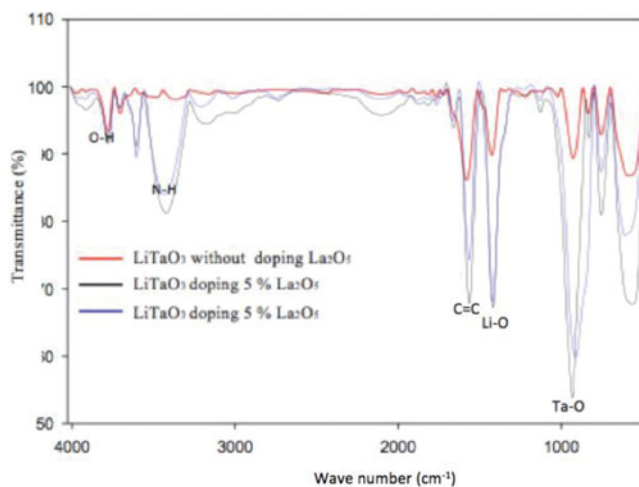


**Figure 2.** The FTIR spectra of  $\text{LiTaO}_3$  thin films.

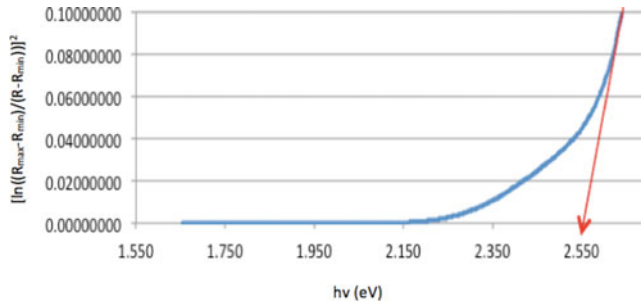


**Figure 3.** Energy gap of undoped thin films.

each of dopant addition. Thus, the absorption value tends to increase with the increasing in dopant concentration.

### 3.3. Optical Analysis

**3.3.1 Energy Gap.** The results show the energy gap of undoped, 5% La doped, and 10% La doped thin films are 2.550 eV, 2.020 eV, and 2.199 eV, respectively (Figs. 3–5). It can be concluded that the higher dopant concentration leads to the lower energy gap, which means the electron will be easier to move from the valence band area into the conduction band.

In this research, the overall values of energy gap of thin films from silicon substrate are in the range of 2.0–3.45 eV for all concentrations. According to other researches, the energy gap of pure silicon is in the range of 1.0–1.3 eV [5–53]. Silicon itself is usually used as semiconductor material and has been applied on many electronic devices for its unique energy gap [56, 57]. In this research, the usage of Si as substrate makes a medium level of energy gap, makes the obtained thin films are capable to be applied in high-voltage electronic components [52].

From the results, it is also found that there is energy gap increasing from 5% to 10% dopant. According to several researches, energy gap can increase after the dopant addition [56–66]. This is the result of Burstein-Moss effect, increasing in band gap value of a thin film-doped semiconductor due to their electrons in the conduction band push the fermi level [67] which lead to the increasing band gap.

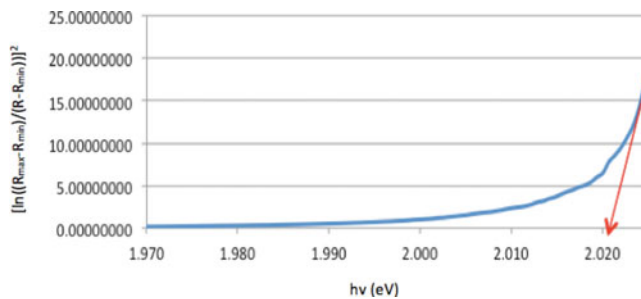


**Figure 4.** Energy gap of 5% lanthanum doped thin films.

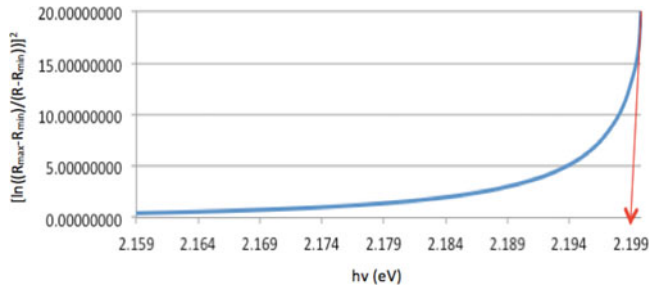


**Figure 5.** Energy gap of 10% lanthanum doped thin films.

**3.3.2 Refractive Index.** The addition of 5% La dopant significantly increases the refractive index from the undoped thin films. However, 10% La dopant decreases the refractive index (Figure 6). Previous researches [68, 69] showed that the refractive index tends to increase with the increasing in dopant concentration, which is caused by the occurrence of disorder in structure, changes in stoichiometry, and internal strain caused by polarizability. Consequently, if containing dopant materials have high polarizability, the refractive index will thus increase [70]. In addition, the phenomenon in dopant increasing decreases the refractive index may be caused by the thinning of the material or the widening of energy gap [71, 72]. From the previously observed energy gaps, it can be seen that there was indeed an increase of energy gap from thin film with 5% dopant to 10% dopant, so that it is likely the cause of decreasing in refractive index.

### 3.4. PSA

To determine the particle size of  $\text{LiTaO}_3$  thin films, particle size analyzer (PSA) device with scale of  $0.6\text{nm} - 7\mu\text{m}$  was used. Figure 7 shows that the  $\text{LiTaO}_3$  thin films have different

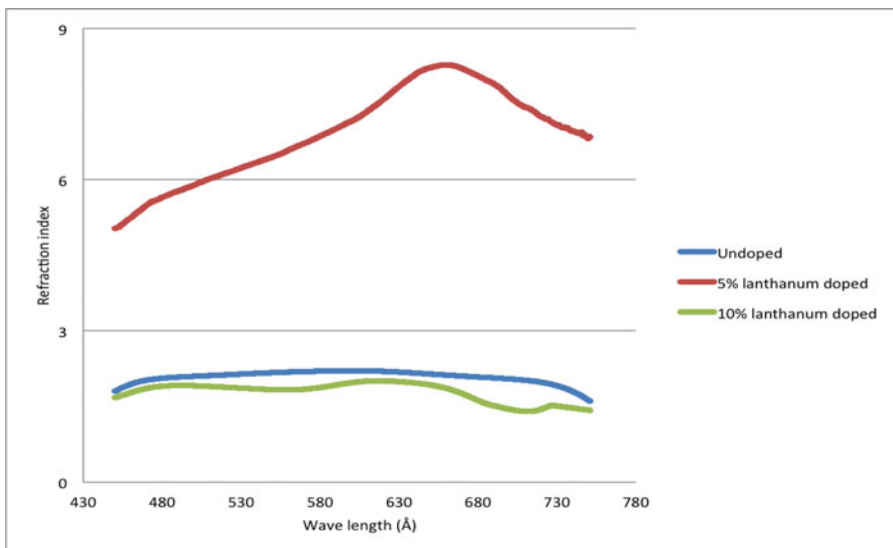


**Figure 6.** Refractive index of undoped, 5% La doped, and 10% La doped  $\text{LiTO}_3$  thin films.

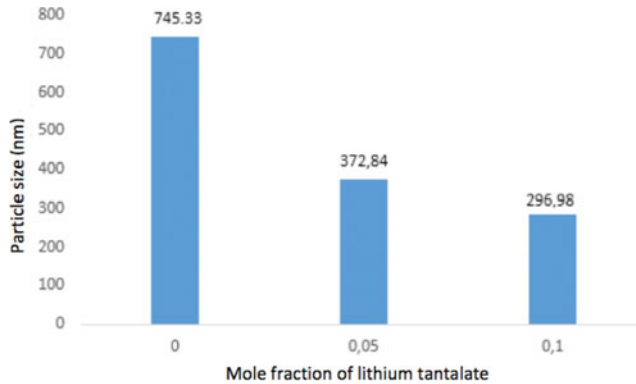


**Figure 7.** The particle size of LiTaO<sub>3</sub> thin films at various mole fractions.

particle sizes. Undoped LiTaO<sub>3</sub> thin films have the largest particle size range, which is 745.33 nm. Meanwhile, the particle size of 5% and 10% La doped LiTaO<sub>3</sub> thin films were 372.84 nm and 296.98 nm, respectively. These results indicate that the higher dopant concentration, the smaller the particle size.

#### 4. Conclusion

The addition of lanthanum dopant ignites the formation of LiTaO<sub>5</sub> crystal, especially in the addition of 10% lanthanum dopant with the hexagonal-shaped crystals. From FTIR, the higher the dopant concentration given, the larger the absorption of Ta-O and Li-O. Moreover, from PSA, it is found that the dopant addition leads to smaller particle size. The optical measurements show that the higher the dopant concentration leads to the lower the energy gap and the higher the refractive index of thin films.

#### Funding

This work was funded by Kerjasama Luar Negeri dan Publikasi Internasional, Kementerian Riset, Teknologi, dan Pendidikan Tinggi, Republik Indonesia under contract No. 082/SP2H/UPL/DIT.LITABMAS/III/2015.

#### REFERENCES

1. J. Kushibiki: Quantitative characterization of proton-exchanged layers in LiTaO<sub>3</sub> optoelectronic devices by line-focus-beam acoustic microscopy. *IEEE Photonic Technology Letters*. **8**(11), 1516–1518 (1996).
2. T. N. Blanton, and H. Liang-Sun: X-ray diffraction characterization of multilayer epitaxial thin films deposited on (0001) sapphire. *The Rigaku Journal*. **13**(1), 3–8 (1996).
3. A. H. M. Gonzalez, A. Z. Simoes, M. A. Zaghete, E. Longo, and J. A. Varela: Effect of thermal treatment temperature on the crystallinity and morphology of LiTaO<sub>3</sub> thin films prepared from polymeric precursor method. *journal of electroceramics*. **13**, 353–359 (2004).
4. V. Y. Shur: Self-organization in LiNbO<sub>3</sub> and LiTaO<sub>3</sub>: formation of micro- and nano-scale domain patterns. *Ferroelectrics*. **304**, 111–116 (2004).
5. Christophis: Adherent cells avoid polarization gradients on periodically poled LiTaO<sub>3</sub> ferroelectrics. *Biointerphases*. **8**(27), 1–9 (2013).

6. A. H. M. Gonzalez, A. Z. Simoes, M. A. Zaghete, and J. A. Varela: Effect of preannealing on the morphology of LiTaO<sub>3</sub> thin films prepared from the polymeric precursor method. *Materials Characterization*. **50**, 233–238 (2003).
7. B. S. Allimi, M. Aindow, and S. P. Alpay: Thickness dependence of electronic phase transitions in epitaxial V<sub>2</sub>O<sub>3</sub> films on (0001) LiTaO<sub>3</sub>. *Applied Physics Letters*. **93**, 109–112 (2008).
8. P. M. Vilarinho, N. Barroca, S. Zlotnik, P. Felix, and M. H. Fernandes: Are lithium niobate (LiNbO<sub>3</sub>) and lithium tantalate (LiTaO<sub>3</sub>) ferroelectrics bioactive? *Materials science and engineering C*. **39**, 395–402 (2014).
9. Y. Tao: Influence of chemical reduction on optical and electrical properties of LiTaO<sub>3</sub> crystal. *Journal of Alloys and Compounds*. **497**, 412–415 (2010).
10. S. Youssel: Characterization of LiTaO<sub>3</sub> thin films fabricated by sol–gel technique. *Microelectronics Journal*. **38**, 63–66 (2007).
11. S. Amir, R. Arsat, H. Xiuli, K. Kalantar-Zadeh, and W. Wlodarski: Polyvinylpyrrolidone/ polyaniline composite based 36° YX LiTaO<sub>3</sub> surface acoustic wave H<sub>2</sub> gas sensor. *Sains Malaysiana*. **42** (2), 213–217 (2013).
12. V. Norkus: Uncooled linear arrays based on LiTaO<sub>3</sub>. *DIAS Infrared GmbH*. **8**, 1–7 (2000).
13. W. Bruce and Wessels: Ferroelectric epitaxial thin films for integrated optics. *The Annual Review Materials Research*. **37**, 659–679 (2007).
14. M. A. Aeagerter: Ferroelectric thin coatings. *Journal of Non-Crystalline Solids*. **151**, 195–202 (1992).
15. D. G. Schlom, C. Long-Qing, P. Xiaoqing, A. Schmehl, and M. A. Zurbuchen: A thin film approach to engineering functionality into oxides. *Journal of American Ceramic Society*. **91** (8), 2429–2454 (2008).
16. V. Stenger, M. Shnider, and S. Sriram: Thin film lithium tantalate (TFLT<sup>TM</sup>) pyroelectric detectors. *Optoelectronic Materials and Devices*. **8** (26), 1–27 (2012).
17. C. C. Chan, M. C. Kao, and Y. C. Chen: Effects of membrane thickness on the pyroelectric properties of LiTaO<sub>3</sub> thin film IR detectors. *Japanese Journal of Applied Physics*. **44**(2), 257–265 (2005).
18. Cassons: Electro-optic coefficients of lithium tantalite at near-infrared wavelengths. *Journal Society of America*. **21**(11), 1948–1952 (2008).
19. M. V. Yakushev, P. Maiello, T. Raadik, M. J. Shaw, P. R. Edwards, J. Krustok, A. V. Mudryi, I. Forbes, and R. W. Martin: Investigation of the structural, optical and electrical properties of Cu<sub>3</sub>Bi<sub>5</sub>S<sub>3</sub> semiconducting thin films. *Energy Procedia*. **60**, 166–172 (2014).
20. H. Saima, Y. Mogi, and T. Haraoka: Development of PSA system for the recovery of carbon dioxide and carbon monoxide from blast furnace gas in steel works. *Energy Procedia*. **37**, 7152–7159 (2013).
21. C. Ketelaar and V. Ajaev: Models of drainage and rupture of thin electrolyte films on flat and structured solid substrates. *Procedia IUTAM*. **15**, 132–138 (2015).
22. R. Chen *et al.* : Percent free prostate-specific antigen for prostate cancer diagnosis in Chinese men with a PSA of 4.0e10.0 ng/mL: results from the Chinese Prostate Cancer Consortium. *Asian Journal of Urology*. **12**, 1–7 (2015).
23. T. Gul, S. Islam, R. A. Shah, I. Khan, and S. Shafie: Analysis of thin film flow over a vertical scillating belt with a second grade fluid. *Engineering Science and Technology, an International Journal*. **18**, 207–217 (2015).
24. P. Capek, G. Stone, V. Dierolf, C. Althouse, and V. Gopalan: Raman studies of ferroelectric domain walls in lithium tantalite and niobate. *Phys Stat Sol.* **4**, 830–833 (2007).
25. P. J. Collings: Simple measurement of the band gap in silicon and germanium. *Am J Phys*. **48** (3):197–199 (1980).
26. J. Millán, P. Godignon, and A. Pérez-Tomás: Wide band gap semiconductor devices for power electronics. *AUTOMATIKA*. **53** (2), 107–116 (2012).
27. G. Panomsuwan, O. Takai, and N. Saito: Optical and mechanical properties of transparent SrTiO<sub>3</sub> thin films deposited by ECR ion beam sputter deposition. *Phys Status Solid A.* ; **210** (2), 311–319 (2013).

28. K. van Benthem, C. Elsässer, and R. H. French: Bulk electronic structure of SrTiO<sub>3</sub> : experiment and theory. *J Appl Phys.* **90**(12), 6156–6174 (2001).
29. D. H. Lee and R. A. Condrate, SR: FTIR spectral characterization of thin film coatings of oleic acid on glasses: I. coatings on glasses from ethyl alcohol. *Journal of Materials Science.* **34**, 139–146 (1999).
30. S. Sathish and B. C. Shekar: Preparation and characterization of nano scale PMMA thin film. *Indian Journal of Pure & Applied Physics.* **52**, 64–67 (2014).
31. W. A. Jabbar, N. F. Habubi, and S. S. Chiad: Optical characterization of silver doped poly (vinyl alcohol) films. *Journal of The Arkansas Academy of Science.* **64**, 101–105 (2010).
32. A. Kassim, S. Nagalingam, S. M. Ho, and N. Karrim: XRD and AFM studies of ZnS thin films produced by electrodeposition method. *Arabian Journal of Chemistry.* **3**, 243–249 (2010).
33. D. Rajesh and C. S. Sunandana: XRD, optical and AFM studies on pristine and partially iodized Ag thin film. *Result in Physics.* **2**, 22–25 (2012).
34. Irzaman, Irmansyah, H. Syahfutra, A. Arif, H. Alatas, Y. Astuti, Siskandar, R Nurullaeli, Aminullah, G.P.A. Sumiarna, Z. A. Z. Jamal: Effect of annealing times for LiTaO<sub>3</sub> thin films on structure, nano scale grain size and band gap. *American Journal of Materials Research.* **1**(1), 7–13 (2014).
35. Irzaman, Y. A. Darvina, P. Fuad, M. Arifin, and Barmawi. M Budiman: Physical and piroelectric properties of tantalum oxide doped lead zirconium titanate Pb<sub>0.995</sub>(Zr<sub>0.525</sub>Ti<sub>0.010</sub>)O<sub>3</sub> thin films and its application for IR sensor. *Physica Status Solidi (a).* **199**(3), 416–424 (2003).
36. Irzaman and M. Barmawi: Crystallography and surface morphology of Ta<sub>2</sub>O<sub>3</sub> doped PZT thin films. *Journal Sains MIPA.* **13**(2), 84–88 (2007).
37. Irzaman and M. Barmawi: Tetragonal to cubic phase transformation in tantalum oxide doped PZT ceramic. *Journal Sains MIPA.* **14**(1), 5–7 (2008).
38. Irzaman, H. Darmasetiawan, H. Hardhienata, M. Hikam, P. Arifin, S. N. Jusoh, S. Taking, Z. Jamal, and M. A. Idris: Surface rougness and grain size characterization of effect of annealing temperature for growth gallium and tantalum doped Ba<sub>0.5</sub>Sr<sub>0.5</sub>TiO<sub>3</sub> thin film. *Journal Atom Indonesia.* **35**(1), 57–67 (2009).
39. Irzaman, H. Syahfutra, H. Darmasetiawan, H. Hardhienata, R. Erviansyah, F. Huriawati, A. Maddu, M. Hikam, and P. Arifin: Electrical properties of photodiode BST thin film doped with ferrium oxide using chemical deposition solution method. *Journal Atom Indonesia.* **37**(3), 133–138 (2011).
40. H. Syahfutra, Irzaman, M. N. Indro, and I. D. M. Subrata: Development of iuxmeter based on BST ferroelectric material. The 4<sup>th</sup> Asian Symposium. American Institute of Physics (AIP) Conference. 2010;1325: 75-78.
41. H. Syahfutra, Irzaman, and I. D. M. Subrata: Integrated visible light sensor based on thin film ferroelectric material BST to microcontroller ATmega 8535. *The International Conference on Materials Science and Technology.* **1**(1), 291–296 (2010).
42. Sucipto, I. Surur, I. Deni, S. Bessie, I. Budiman, H. Syahfutra, Irzaman, T. Djatna, T. T. Irawadi, and A. M. Fauzi: Photodiode Ba<sub>0.5</sub>Sr<sub>0.5</sub>TiO<sub>3</sub> thin film as light sensor. *The International Conference on Materials Science and Technology.* **1**(1), 287–290 (2010).
43. A. Ismangil, R. P. Jenie, and Irzaman. Irmansyah: Development of lithium tantalite (LiTaO<sub>3</sub>) for automatic switch on LAPAN-IPB satellite infra-red sensor. *Procedia Environmental Sciences.* **24**, 329–334 (2015).
44. A. Kurniawan, D. Yosman, A. Arif, J. Juansah, and Irzaman: Development and application of Ba<sub>0.5</sub>Sr<sub>0.5</sub>TiO<sub>3</sub> (BST) thin film as temperature sensor for satellite technology. *Procedia Environmental Sciences.* **24**, 335–339 (2015).
45. Z. R. Khan, M. S. Khan, M. Zulfequar, and M. S. Khan: Optical and structural properties of ZnO thin films fabricated by sol-gel method. *Materials Sciences and Applications.* **2**, 340–345 (2011).
46. M. Bouroushian, and T. Kosanovic: Characterization of thin films by low incidence X-Ray Diffraction. *Crystal Structure Theory and Application.* **1**, 35–39 (2012).
47. R. D. Tarey, R. S. Rastogi, and K. L. Chopra: Characterization of thin films by glancing incidence X-Ray Diffraction. *The Rigaku Journal.* **4**(1), 11–15 (1987).

48. X. Fan, X. Shen, A. Q. Liuc, and J. Kuo: Band gap opening of graphene by doping small boron nitride domains. *Nanoscale*. **4**, 2157–2165 (2012).
49. K. van Benthem and C. Elsässer: Bulk electronic structure of SrTiO<sub>3</sub>: Experiment and theory. *Journal of Applied Physics*. **90**(12), 6156–6164 (2001).
50. N. Serpone: Is the band gap of pristine TiO<sub>2</sub> narrowed by anion- and cation-doping of titanium dioxide in second-generation photocatalysts? *J. Phys. Chem.* **110**, 24287–24293 (2006).
51. P. J. Collings: Simple measurement of the band Gap in silicon and germanium. *A. J. Phys.* **48**(3), 197–199 (1980).
52. J. Millán, P. Godignon, and A. P. Tomás: Wide band gap semiconductor devices for power electronics. *AUTOMATIKA*. **53**(2), 107–116 (2012).
53. B. G. Streetman: *Solid State Electronic Devices*. Michigan (US): Prentice Hall; (1995).
54. W. C. O'Mara, R. B. Herring, and L. P. Hunt: *Handbook of Semiconductor Technology*. Saddle River (US): Noyes Publications; (1990).
55. Y. Nishi and R. Doering: *Handbook of Semiconductor Manufacturing Technology*, 2<sup>nd</sup> ed. Boca Raton (US): CRC Press; (2007).
56. J. D. Cressler: *Circuits and Applications Using Silicon Heterostructure Devices*. London: CRC Press; (2007).
57. A. C. Diebold: *Handbook of Silicon Semiconductor Metrology*. Boca Raton: CRC Press; (2001).
58. W. Zhu, X. Qui, V. Iancu, X. Q. Chen, H. Pan, W. Wang, N. M. Dimitrijevic, T. Rajh, H. M. Meyer, M. P. Paranthaman, G. M. Stocks, H. H. Weitering, B. Gu, G. Eres, and Z. Zhang: Band gap of narrowing titanium oxide semiconductors by noncompensated anion-cation codoping for enhanced visible-light photoactivity. *Phys Rev Lett*. **103**(22), 226401-1–226401-4 (2009).
59. A. S. Ahmed, M. Shafeeq, and M. Singla: Band gap narrowing and fluorescence properties of nickel doped SnO<sub>2</sub> nanoparticles. *J Luminescence*. **131**, 1–6 (2011).
60. M. Chakraborty, A. Ghosh, and R. Thangavel: Experimental and theoretical investigations of structural and optical properties of copper doped ZnO nanorods. *J Sol-Gel Sci Technol*. **74**, 756–764 (2015).
61. H. J. Lee, S. Y. Jeong, C. R. Cho, and C. H. Park: Study of diluted magnetic semiconductor: Co-doped ZnO. *Appl Phys Lett*. **81**(21), 4020–4022 (2002).
62. J. Chu and A. Sher: *Physics and Properties of Narrow Gap Semiconductors (Microdevices)*. New York: Springer; (2008).
63. I. Hamberg, C. G. Granqvist, K. F. Berggren, B. E. Sernelius, and L. Engström: Band-gap widening in heavily Sn-doped In<sub>2</sub>O<sub>3</sub>. *Phys Rev B Condens Matter*. **30**(6), 3240 (1984).
64. J. Wu, W. Walukiewicz, W. Shan, K. M. Yu, III, J. W. Ager, E. E. Haller, H. Lu, and W. J. Schaff: Effects of the narrow band gap on the properties of InN. *Phys Rev B*. **66**, 201403-1–201403-4 (2002).
65. A. Jain, P. Sagar, and R. M. Mehra: Band gap widening and narrowing in moderately and heavily doped n-ZnO films. *Solid-State Electronics*. **50**, 1420–1424 (2006).
66. A. Walsh, J. L. F.D Silva, and S. H. Wei: Origins of band-gap renormalization in degenerately doped semiconductors. *Phys Rev B*. **78**(7), 075211-1–075211-5 (2008).
67. J. S. Manser and P. Kamat: Band filling with free charge carriers in organometal halide perovskites. *Nature Photonics*. **8**(9), 737–743 (2014).
68. O. V. Butov, K. M. Golant, A. L. Tomashuk, M. J. N. van Stralen, and A. H. E. Breuls: Refractive index dispersion of doped silica for fiber optics. *Optics Comm*. **213**, 301–308 (2002).
69. T. J. Alwan: Refractive index dispersion and optical properties of dye-doped polystyrene films. *Malaysian Polymer J*. **5**(2), 204–213 (2010).
70. P. Sharma and S. C. Katyal: Linear and nonlinear refractive index of As-Se-Ge and Bi doped As-Se-Ge thin films. *J Appl Phys*. **107**(11), 113527 (2010).
71. C. M. Krowne and Y. Zhang: *Physics of Negative Refraction and Negative Index Materials*. New York: Springer; (2007).
72. M. Hotoleanu: *Highly Doped Fiber Technology*. In: Thévenaz L, ed. *Advanced Fiber Optics: Concepts and Technology*. Lausanne: EFPL Press; 127–144 (2011).